ELSEVIER

International Journal of Minerals, Metallurgy and Materials
Volume 16, Number 6, December 2009, Page 696

Materials

Enhancement of magnetic properties and thermal stability of nanocrystalline $(NdDyTb)_{12.3}(FeZrNbCu)_{81.7}B_{6.0}$ alloy with Co substitution

Xiao-qian Bao[1)], Wei Li[2)], Jie Zhu[1)], Xue-xu Gao[1)], and Shou-zeng Zhou[1)]

1) State Key Laboratory for Advanced Metals and Materials, University of Science and Technology Beijing, Beijing 100083, China
2) College of Materials Science and Engineering, Yanshan University, Qinhuangdao 066004, China
(Received 2008-10-30)

Abstract: The major drawbacks of Nd-Fe-B magnets are relatively low Curie temperature and poor thermal stability. Ribbons with the near stoichiometric 2:14:1 composition of $Nd_{10.8}Dy_{0.75}Tb_{0.75}Fe_{79.7-x}Co_xZr_{0.8}Nb_{0.8}Cu_{0.4}B_{6.0}$ (x=0, 3, 6, 9, 12, 15) were prepared by rapid quenching and subsequent heat treatment. The effect of Co element on the magnetic properties, thermal stability, and microstructure of the ribbons was systematically studied by vibrating sample magnetometer (VSM), thermal magnetic analysis, atomic force microscopy (AFM), and transmission electron microscopy (TEM). It was found that Co substitution was significantly effective in improving the magnetic properties and the thermal stability of nanocrystalline ribbons. Although the intrinsic coercivity decreased from 1308.7 kA/m for x=0 to 817.4 kA/m for x=15, the remanence polarization and maximum energy product increased from 0.839 T and 116.5 kJ/m^3 for the Co-free samples to 1.041 T and 155.1 kJ/m^3 for the 12at% Co-substituted samples, respectively. About 10 K increase in Curie temperature was observed for the 2:14:1 phase with 1at% Co substitution. The absolute values of temperature coefficients of induction and coercivity were significantly decreased with Co substitution, which may be attractive for high operational temperature applications. The microstructure of nanocrystalline ribbons was slightly refined with Co substitution.

Key words: nanocrystalline magnets; Nd-Fe-B magnets; Co substitution; magnetic properties; thermal stability; microstructure

1. Introduction

Remanence enhancement in nanocomposite magnets is well known to be related to the exchange coupling between magnetically soft and hard phases, which provides us a new way to develop novel permanent magnets with high performance [1-4]. However, the presence of soft phase increases the remanence polarization J_r but decreases the coercivity H_{ci}, so that their application is limited [5]. Alloys with the Nd content higher than 11at%, *i.e.*, close to the stoichiometry composition of $Nd_2Fe_{14}B$, are being studied to further improve the coercivity [6]. The major drawbacks of Nd-Fe-B magnets are relatively low Curie temperature (T_c) and poor thermal stability, which limit the useful operating temperatures of commercial magnets. To improve the thermal stability of Nd-Fe-B magnets, extensive efforts have been made *via* the substitution of other elements [7-8]. It has been found that, among all the substitutions studied, Co substitution appears to be an effective way to improve the thermal stability in sintered Nd-Fe-B magnets [9] and in nanocomposite α-Fe/$Nd_2Fe_{14}B$ magnets [10-13]. Meanwhile, many experimental results have shown that a moderate Co substitution for Fe can increase the saturation magnetization of Nd-Fe-B magnets [14-15]. Thus, this study is focused on the influence of Co addition on the magnetic properties and thermal stability of the near stoichiometric $(NdDyTb)_{12.3}(FeZrNbCu)_{81.7}B_{6.0}$ alloy, aiming at understanding the role of Co addition in nanocrystalline magnets, which would shed some lights on the future design of nanocrystalline magnets for scientific inquiry and industrial applications.

2. Experimental procedures

Alloy ingots with the nominal composition of $Nd_{10.8}Dy_{0.75}Tb_{0.75}Fe_{79.7-x}Co_xZr_{0.8}Nb_{0.8}Cu_{0.4}B_{6.0}$ (x=0, 3, 6, 9, 12, 15) were prepared by arc melting the pure constituent elements under high-purity atmosphere. The ingots were melted four times to ensure homogeneity. After being crushed, small pieces of about 6-8 g each to accommodate the size of the crucible were used for melt spinning. 2-3 mm wide and 30-60 μm thick ribbons were obtained by ejecting the molten al-

Corresponding author: Xiao-qian Bao, **E-mail:** bxq118@skl.ustb.edu.cn

Also available online at www.sciencedirect.com

loys from a quartz tube with an orifice diameter of about 0.6 mm onto a copper wheel at the surface speed (V_s) of 22 m/s. These amorphous flakes were then sealed in a quartz tube under the vacuum of 2×10^{-3} Pa and annealed at 550-750°C for 10 min to crystallize and develop a desired fine nanoscale microstructure and optimize the coercivity. Room temperature hysteresis loops of the ribbons were measured using a LDJ 9600 vibrating sample magnetometer (VSM) with an applied field up to 1600 kA/m. The length direction of the ribbons was parallel to the applied field to minimize the demagnetization effect. The thermal magnetic data (magnetic pole strength *m vs*. temperature *T*) and demagnetization curves from room temperature up to 400°C were measured using a LakeShore 7407 VSM with an applied field up to 1200 kA/m. The Curie temperature T_c was determined from the *m*-*T* curves by drawing a tangent line to the transition step and finding the temperature value of its intersection with the extended baseline. The temperature-dependent magnetic properties were characterized by the temperature coefficients of $m_r(\alpha)$ and $H_{ci}(\beta)$, defined, respectively, as $\alpha=[m_r(T_1)-m_r(T_2)]/[m_r(T_1)\times(T_1-T_2)]\times100\%$ and $\beta=[H_{ci}(T_1)-H_{ci}(T_2)]/[H_{ci}(T_1)\times(T_1-T_2)]$. Microstructural studies were characterized by atomic force microscopy (AFM) and transmission electron microscopy (TEM). AFM observation was made on the free surface of the ribbons with no further surface preparation. The thin foils for TEM observation were made by Ar-ion beam polishing.

3. Results and discussion

3.1. Enhancement of magnetic properties at room temperature

Fig. 1 shows the typical hysteresis loops of the $Nd_{10.8}Dy_{0.75}Tb_{0.75}Fe_{79.7-x}Co_xZr_{0.8}Nb_{0.8}Cu_{0.4}B_{6.0}$ melt-spun ribbons prepared at the wheel speed of 22 m/s. It is clear that permanent magnetic properties of the melt-spun ribbons decrease drastically with increasing Co content. The demagnetization curves are smooth and show good squareness for the x=0-6 samples but show a very low coercivity and the distinct kink for the $x\geq9$ samples. This indicates that Co addition improves significantly the amorphousizing tendency of the $Nd_{10.8}Dy_{0.75}Tb_{0.75}Fe_{79.7-x}Co_xZr_{0.8}Nb_{0.8}Cu_{0.4}B_{6.0}$ alloy since the shapes of hysteresis loops are very sensitive to microstructure. It also means that the optimal wheel speeds shift to low values with increasing Co content.

Since the amorphous phase is undesired, to obtain the optimal magnetic properties for the samples with different Co contents, thermal treatment was used individually to the quenched ribbons to induce a fine grain structure crystallizing from the amorphous state. Figs. 2 and 3 show the typical hysteresis loops and variation of saturation polarization J_s, remanence polarization J_r, intrinsic coercivity H_{ci}, and maximum energy product $(BH)_{max}$ with the Co content of $Nd_{10.8}Dy_{0.75}Tb_{0.75}Fe_{79.7-x}Co_xZr_{0.8}Nb_{0.8}Cu_{0.4}B_{6.0}$ ribbons optimally annealed, respectively. X-ray diffraction analysis reveals single-phase materials. All the ribbons have a high saturation remanence ratio of about 0.75, suggesting the existence of the intergranular exchange-coupling effect in all samples, which is similar to the typical nanocomposite magnet. J_s and J_r increase with the increase in Co content x up to 12 and then decrease for x=15 mainly because of the formation of $Nd_2(Fe,Co)_{17}$ phase [11-12]. H_{ci} of the optimally processed ribbons decreases from 1308.7 kA/m for x=0 to 817.4 kA/m for x=15, which can be explained by the lower anisotropic field of $Nd_2Co_{14}B$ (μ_0H_A=5.5 T) than that of $Nd_2Fe_{14}B$ (μ_0H_A=7.3 T). The variation of $(BH)_{max}$ with Co content is consistent with that of J_s and J_r. The optimum magnetic properties with J_r=1.041 T, H_{ci}=944.9 kA/m, and $(BH)_{max}$=155.1 kJ/m^3 were achieved for the x=12 ribbons.

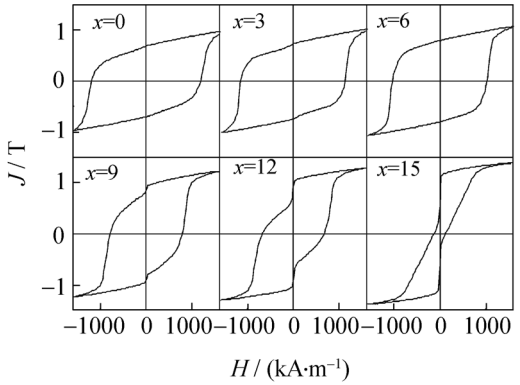

Fig. 1. Hysteresis loops of the $Nd_{10.8}Dy_{0.75}Tb_{0.75}Fe_{79.7-x}Co_xZr_{0.8}Nb_{0.8}Cu_{0.4}B_{6.0}$ ribbons prepared at the wheel speed of 22m/s.

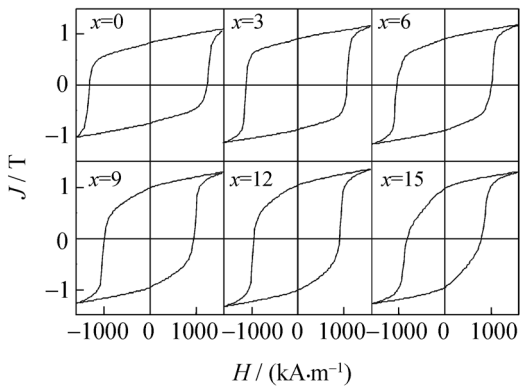

Fig. 2. Hysteresis loops of the $Nd_{10.8}Dy_{0.75}Tb_{0.75}Fe_{79.7-x}Co_xZr_{0.8}Nb_{0.8}Cu_{0.4}B_{6.0}$ ribbons optimally annealed.

3.2. Improvement in thermal stability

Fig. 4 shows the $m(T)$ curves for the $Nd_{10.8}Dy_{0.75}Tb_{0.75}Fe_{79.7-x}Co_xZr_{0.8}Nb_{0.8}Cu_{0.4}B_{6.0}$ (x=0, 6, 12) ribbons. It can be seen that the Curie temperature T_c of the 2:14:1 phase increases from 338.7°C for x=0 to 443.6°C for x=12. An increase in T_c for the 2:14:1 phase with Co addition can be explained by a preferential substitution of Co into Fe sites involved in anti-ferromagnetic interactions. By reducing a fraction of the negative exchange interactions, the overall exchange becomes stronger, thus enhancing T_c. This suggests that Co may, presumably, enter the crystal structure of the 2:14:1 phase. The Co content dependence of T_c for the 2:14:1 phase is in good agreement with the results reported for nanocrystalline Nd-Fe-B melt-spun alloys that each 1at% Co substitution for Fe produces about a 10°C increase in T_c [16].

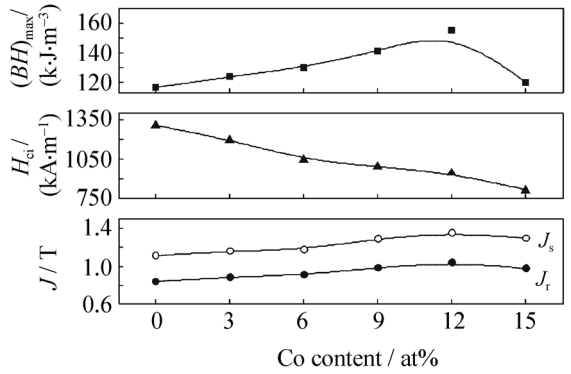

Fig. 3. Dependence of J_s, J_r, H_{ci}, and $(BH)_{max}$ of the $Nd_{10.8}Dy_{0.75}Tb_{0.75}Fe_{79.7-x}Co_xZr_{0.8}Nb_{0.8}Cu_{0.4}B_{6.0}$ ribbons optimally annealed on Co content.

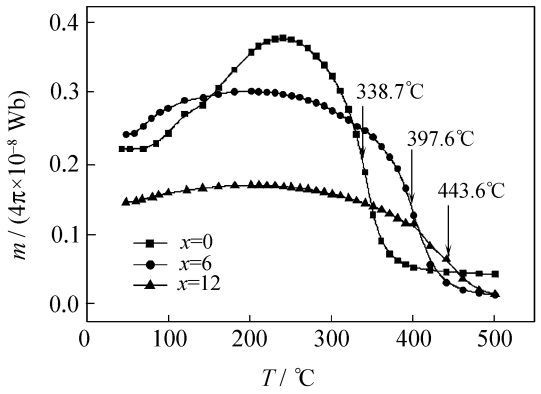

Fig. 4. m-T curves and temperature dependence of magnetic pole strength for the $Nd_{10.8}Dy_{0.75}Tb_{0.75}Fe_{79.7-x}Co_xZr_{0.8}Nb_{0.8}Cu_{0.4}B_{6.0}$ ribbons.

Fig. 5 shows hysteresis loops of the x=0, 6, and 12 ribbons measured from 25°C up to 400°C. It can be seen that the permanent magnetic properties of all the samples decrease significantly with increasing temperature, but the high temperature magnetic properties of the ribbons are strongly dependent on Co substitution. To clearly demonstrate the effect of Co substitution on the temperature dependence of m_r and H_{ci}, Fig. 6 was constructed using the data obtained from Fig. 5.

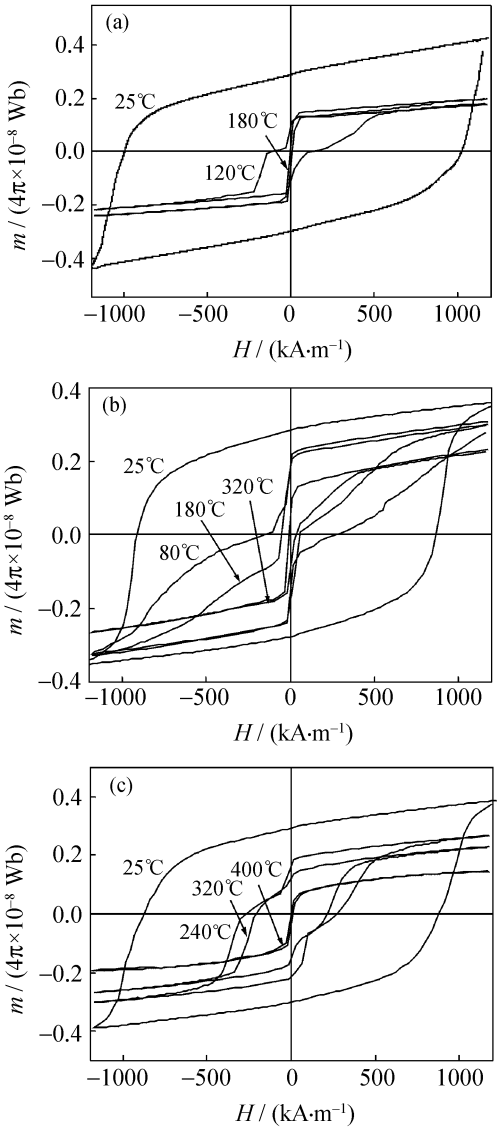

Fig. 5. Hysteresis loops measured from 25°C up to 400°C for the x=0 (a), x=6 (b), and x=12 (c) ribbons.

It is clear that both m_r and H_{ci} decrease significantly with increasing temperature. However, the decrease rates are affected by Co substitution. For example, under the applied field of 1200 kA/m, the intrinsic coercivity of the x=0 sample with the coercivity of 993 kA/m is much higher than that of the x=6 sample with the coercivity of 909 kA/m at 25°C, but H_{ci} for the x=0 sample is much lower than that of the x=6 sample at 180°C. Meanwhile, the coercivities of 269 kA/m and 209 kA/m are obtained for the x=12 sample at 240 and 320°C, respectively. As shown in Fig. 7, the temperature coefficient of m_r and the temperature coefficient of H_{ci} exhibit a significant decrease (in absolute value) with Co substitution. The decrease in α can be attributed to the increase in Curie temperature with Co substitution. The change in β with the Co content may be attributed to the change of microstructure and tem-

perature dependence of the anisotropy field (H_A) of the 2:14:1 phase with Co substitution, which requires further investigation.

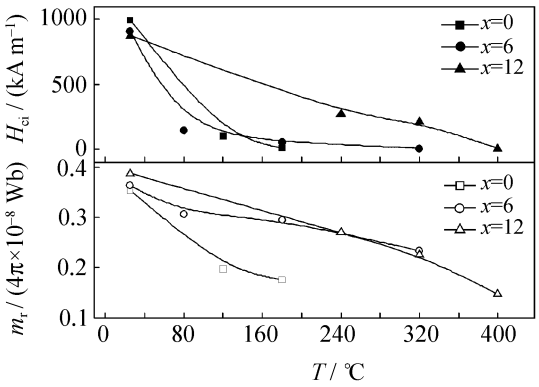

Fig. 6. Variation of coercivity and remanence with temperature for the x=0, 6, and 12 ribbons.

3.3. Microstructure evaluation

To better understand the effect of Co addition on microstructure, AFM and TEM were used to image the microstructure of the surface and inner parts of the ribbons and determine the $Nd_2Fe_{14}B$ grain size and grain size distribution. Figs. 8 and 9 show the AFM and TEM images of the x=0 and x=12 ribbons annealed at 675°C for 10 min for comparison, respectively. From these figures, the Co-free sample shows an average grain size of around 80 nm, slightly coarser than the grain size of 70 nm for the 12at% Co-substituted sample. Because of the presence of finer particles, TEM diffraction patterns are composed of continuous small circular spots.

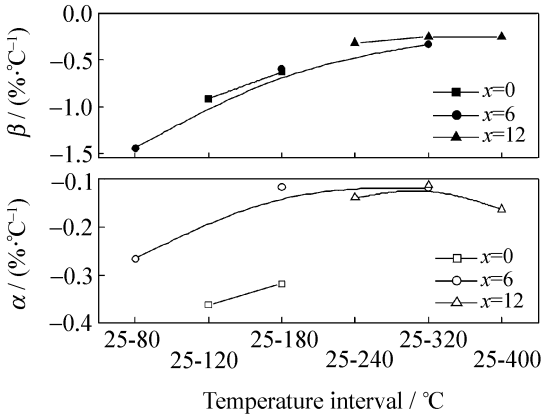

Fig. 7. Temperature coefficients of coercivity (β) and remanent magnetic pole strength (α) of the x=0, 6, and 12 ribbons as a function of Co content.

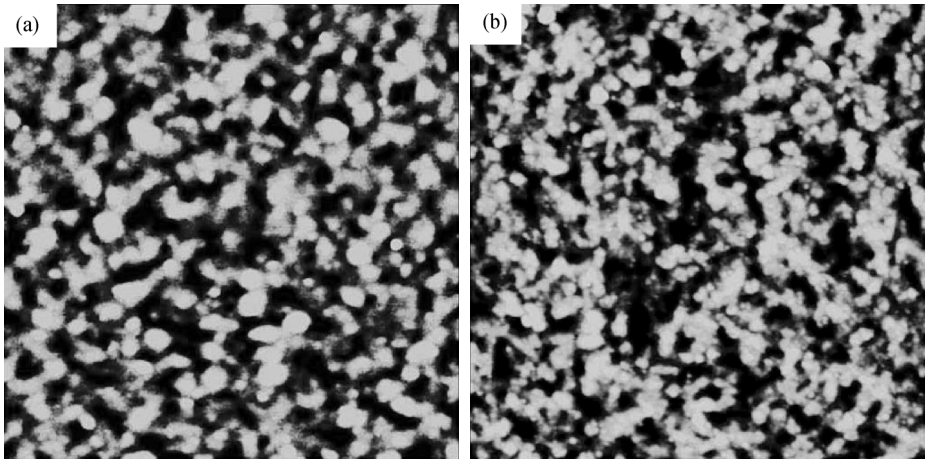

Fig. 8. AFM images of the ribbons annealed at 675°C for 10 min: (a) x=0; (b) x=12.

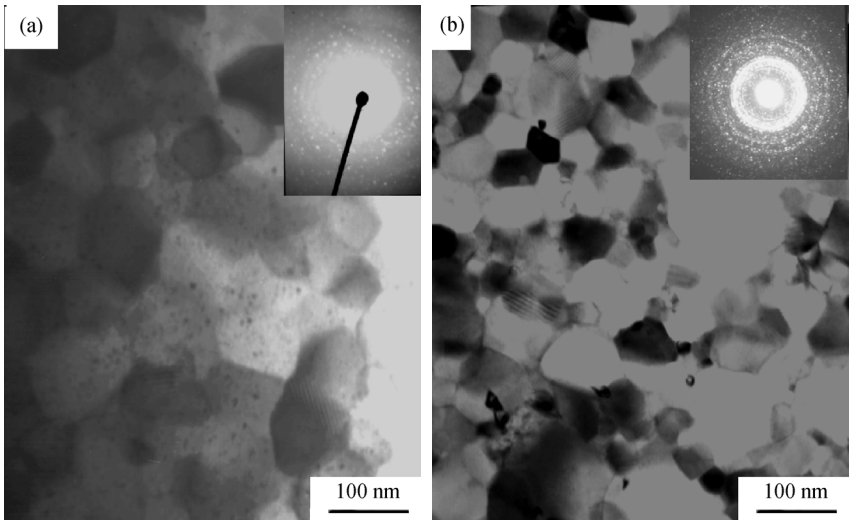

Fig. 9. TEM images and electron diffraction patterns of the ribbons annealed at 675°C for 10 min: (a) x=0; (b) x=12.

4. Conclusions

(1) For the $Nd_{10.8}Dy_{0.75}Tb_{0.75}Fe_{79.7-x}Co_xZr_{0.8}Nb_{0.8}Cu_{0.4}B_{6.0}$ (x=0-15) nanocrystalline ribbons, although the intrinsic coercivity H_{ci} decreases from 1308.7 kA/m for x=0 to 817.4 kA/m for x=15, the remanence polarization J_r and maximum energy product $(BH)_{max}$ increase from 0.839 T and 116.5 kJ/m^3 for the Co-free samples to 1.041 T and 155.1 kJ/m^3 for the 12at% Co-substituted samples, respectively.

(2) Co substitution for Fe in nanocrystalline Nd-Fe-B ribbons leads to an increase in T_c of the 2:14:1 phase and a decrease in absolute values of temperature coefficients of induction and coercivity, which may be attractive for high operational temperature applications.

(3) The microstructure of nanocrystalline ribbons is slightly refined with Co substitution.

References

[1] X.Q. Bao, Y. Qiao, X.X. Gao, *et al.*, Effect of annealing time on exchange coupling interactions and microstructure of nanocomposite $Pr_{7.5}Dy_1Fe_{71}Co_{15}Nb_1B_{4.5}$ ribbons, *J. Univ. Sci. Technol. Beijing*, 14 (2007), No.6, p.547.

[2] T. Ohkubo, T. Miyoshi, S. Hirosawa, *et al.*, Effects of C and Ti additions on the microstructures of $Nd_9Fe_{77}B_{14}$ nanocomposite magnets, *Mater. Sci. Eng. A*, 449-451(2007), p.435.

[3] Z.W. Liu and H.A. Davies, The practical limits for enhancing magnetic property combinations for bulk nanocrystalline NdFeB alloys through Pr, Co and Dy substitutions, *J. Magn. Magn. Mater.*, 313(2007), p.337.

[4] C. Wang, M. Yan, and W.Y. Zhang, Significant changes in the microstructure, phase transformation and magnetic properties of (Nd, Pr)$_2$Fe$_{14}$B/α-Fe magnets induced by Nb and Zr additions, *Mater. Sci. Eng. B*, 123(2005), p.80.

[5] L.G. Pampillo, F.D. Saccone, and H.R.M. Sirkin, Structural and magnetic properties of nanocrystalline $Nd_{4.5}Fe_{72}Co_2Cr_3Al_1B_{17.5}$ ribbons, *Phys. B*, 389(2007), p.172.

[6] Y.L. Tang, M.J. Kramer, K.W. Dennis, *et al.*, On the control of microstructure in rapidly solidified Nd-Fe-B alloys through melt treatment, *J. Magn. Magn. Mater.*, 267(2003), p.307.

[7] Z.M. Chen, Y.Q. Wu, M.J. Kramer, *et al.*, A study on the role of Nb in melt-spun nanocrystalline Nd-Fe-B magnets, *J. Magn. Magn. Mater.*, 268(2004), p.105.

[8] R. Zhang, Y. Liu, J.W. Ye, *et al.*, Effect of Nb substitution on the temperature characteristics and microstructures of rapid-quenched NdFeB alloy, *J. Alloys Compd.*, 427(2007), p.78.

[9] R.S. Mottram, A.J. Williams, and I.R. Harris, Blending additions of cobalt to $Nd_{16}Fe_{76}B_8$ milled powder to produce sintered magnets, *J. Magn. Magn. Mater.*, 217(2000), p.27.

[10] Z.W. Liu and H.A. Davies, Elevated temperature study of nanocrystalline (Nd/Pr)-Fe-B hard magnetic alloys with Co and Dy additions, *J. Magn. Magn. Mater.*, 290-291(2005), p.1230.

[11] T. Nishio, S. Koyama, Y. Kasai, *et al.*, Low rare-earth Nd-Fe-B bonded magnets with improved irreversible flux loss, *J. Appl. Phys.*, 81(1997), p.4447.

[12] H. Chiriac and M. Marinescu, Magnetic properties of $Nd_8Fe_{77}Co_5B_6CuNb_3$ melt-spun ribbons, *J. Appl. Phys.*, 83(1998), p.6628.

[13] M. Jurczyk and J. Jakubowicz, Improved temperature and corrosion behaviour of nanocomposite $Nd_2(Fe,Co,M)_{14}B$/α-Fe magnets, *J. Alloys Compd.*, 311(2000), p.292.

[14] W.Y. Zhang, A.R. Yan, H.W. Zhang, *et al.*, Effect of the substitution of Co for Fe on phase components and magnetic properties of melt-spun $Pr_9Fe_{85}B_5$ nanocomposites, *J. Alloys Compd.*, 315(2001), p.174.

[15] W.Y. Zhang, H.W. Chang, C.H. Chiu, *et al.*, Beneficial effect of the substitution of Co for Fe on the magnetic properties of melt-spun $Pr_2Fe_{14}C$/α-Fe-type nanocomposite magnets, *J. Alloys Compd.*, 379(2004), p.28.

[16] A. Melsheimer, M. Seeger, and H. Kronmüller, Influence of Co substitution in exchange coupled NdFeB nanocrystalline permanent magnets, *J. Magn. Magn. Mater.*, 202(1999), p.458.